THE JOURNAL OF BIOLOGICAL CHEMISTRY VOL. 286, NO. 4, pp. 2843–2852, January 28, 2011
Printed in the U.S.A.

Oxidative Inactivation of the Lipid Phosphatase Phosphatase and Tensin Homolog on Chromosome Ten (PTEN) as a Novel Mechanism of Acquired Long QT Syndrome*[S]

Received for publication, March 20, 2010, and in revised form, October 23, 2010 Published, JBC Papers in Press, November 20, 2010, DOI 10.1074/jbc.M110.125526

Xiaoping Wan[‡], Adrienne T. Dennis[‡], Carlos Obejero-Paz[§], Jeffrey L. Overholt[¶], Jorge Heredia-Moya[‖], Kenneth L. Kirk[‖], and Eckhard Ficker[‡1]

From the [‡]Rammelkamp Center for Education and Research, MetroHealth Campus, Case Western Reserve University, Cleveland, Ohio 44109, the [§]Department of Physiology and Biophysics, Case Western Reserve University, Cleveland, Ohio 44106, the [¶]Department of Life Sciences, Winston-Salem State University, Winston-Salem, North Carolina 27110, and the [‖]Laboratory of Bioorganic Chemistry, NIDDK, National Institutes of Health, Bethesda, Maryland 20892

The most common cause of cardiac side effects of pharmaco-therapy is acquired long QT syndrome, which is characterized by abnormal cardiac repolarization and most often caused by direct blockade of the cardiac potassium channel human ether a-go-go-related gene (hERG). However, little is known about therapeutic compounds that target ion channels other than hERG. We have discovered that arsenic trioxide (As_2O_3), a very potent antineoplastic compound for the treatment of acute promyelocytic leukemia, is proarrhythmic via two separate mechanisms: a well characterized inhibition of hERG/I_{Kr} trafficking and a poorly understood increase of cardiac calcium currents. We have analyzed the latter mechanism in the present study using biochemical and electrophysiological methods. We find that oxidative inactivation of the lipid phosphatase PTEN by As_2O_3 enhances cardiac calcium currents in the therapeutic concentration range via a PI3Kα-dependent increase in phosphatidylinositol 3,4,5-triphosphate (PIP_3) production. In guinea pig ventricular myocytes, even a modest reduction in PTEN activity is sufficient to increase cellular PIP_3 levels. Under control conditions, PIP_3 levels are kept low by PTEN and do not affect calcium current amplitudes. Based on pharmacological experiments and intracellular infusion of PIP_3, we propose that in guinea pig ventricular myocytes, PIP_3 regulates calcium currents independently of the protein kinase Akt along a pathway that includes a secondary oxidation-sensitive target. Overall, our report describes a novel form of acquired long QT syndrome where the target modified by As_2O_3 is an intracellular signaling cascade.

Combination therapy with As_2O_3 and retinoic acid is so effective in the treatment of acute promyelocytic leukemia that it has the potential to become the standard of care in patients (1–3). Therapy with As_2O_3 has also shown great promise in additional hematological malignancies and even solid tumors (4). Therefore, it is of the utmost importance to acknowledge that therapeutic use of As_2O_3 can be complicated by cardiotoxicity, including a significant prolongation of the QT interval on the electrocardiogram and an increased propensity to develop torsades de pointes arrhythmias, which may degenerate into fatal ventricular fibrillation (5–7).

Clinically, As_2O_3-induced QT prolongation and torsades de pointes arrhythmias are considered hallmarks for drug-induced or acquired long QT syndrome (acLQTS).[2] In most instances, acLQTS is caused by a direct blockade of the cardiac potassium channel hERG/I_{Kr}, which is crucial for terminal repolarization of the cardiac action potential (8). Importantly, this is not the case for As_2O_3-induced long QT syndrome. Instead, we have discovered that antineoplastic As_2O_3 is proarrhythmic 1) by inhibition of hERG export to the cell surface via disruption of channel-chaperone interactions essential for hERG maturation and 2) by a fast increase in cardiac calcium currents (9). Just like hERG block or hERG trafficking inhibition, increases in cardiac calcium currents have been implicated in prolongation of the cardiac action potential as well as the induction of early and delayed afterdepolarizations (10, 11). However, it remains unknown by what mechanisms As_2O_3 increases cardiac calcium currents. Here it is our main goal to identify the molecular target(s) underlying As_2O_3-induced modulation of cardiac calcium currents.

In general, it is thought that As_2O_3 compromises cellular functions through binding to sulfhydryl groups and the generation of reactive oxygen species (12). We report here that exposure to As_2O_3 inactivates the "phosphatase and tensin homolog on chromosome ten" (PTEN), in cardiac myocytes by direct oxidation of an active site cysteine residue. PTEN is a lipid phosphatase that controls breakdown of the bioactive lipid PIP_3, which is generated from PIP_2 via phosphatidylinositol 3-kinase (PI3K)-dependent phosphorylation (13). Cellu-

* This work was supported, in whole or in part, by National Institutes of Health Grant HL71789 (to E. F.) and intramural funds of NIDDK, National Institutes of Health (to J. H.-M. and K. L. K.). This work was also supported by a grant from the American Heart Association (to J. L. O.).

[S] The on-line version of this article (available at http://www.jbc.org) contains supplemental Figs. S1–S7.

[1] To whom correspondence should be addressed: Rammelkamp Center, MetroHealth Medical Center, 2500 MetroHealth Dr., Cleveland, OH 44109. Tel.: 216-778-8977; Fax: 216-778-8282; E-mail: eficker@metrohealth.org.

[2] The abbreviations used are: acLQTS, acquired long QT syndrome; hERG, human ether a-go-go-related gene; I_{Kr}, rapidly activating delayed rectifier potassium current; PTEN, phosphatase and tensin homolog on chromosome 10; PIP_3, phosphatidylinositol 3,4,5-triphosphate; PIP_2, phosphatidylinositol 4,5-biphosphate; PTP, protein-tyrosine phosphatase; IGF, insulin-like growth factor; NAC, *N*-acetyl cysteine; BisI, bisindolylmaleimide; PKA, protein kinase A; PI, phosphatidylinositol; PI-3P, phosphatidylinositol 3-phosphate.

lar PIP_3 levels have been previously linked to the modulation of L-type ($Ca_v1.2$) calcium currents (*e.g.* in vascular myocytes, in neurons, and in cardiac myocytes) (14–17). We propose that oxidative inactivation of PTEN increases the gain in PI3K-dependent signaling pathways that translate an increase in PIP_3 levels into elevated calcium current amplitudes. This report represents a novel form of acLQTS that is not tied directly to an ion channel or a closely associated protein. Instead, the target modified by the therapeutic compound is a redox-sensitive enzyme far removed from the ion channel and coupled only via an intricate sequence of intracellular signaling events.

EXPERIMENTAL PROCEDURES

Cellular Electrophysiology—Single ventricular myocytes were isolated from adult guinea pigs as described previously (18). Cardiac calcium currents were recorded at room temperature (20–22 °C) using the whole cell patch clamp technique. The extracellular bath solution contained Tyrode's solution (137 mM NaCl, 5.4 mM CsCl, 1.8 mM $MgCl_2$, 1.8 mM $CaCl_2$, 10 mM glucose, 10 mM HEPES (pH 7.4). Patch pipettes were filled with 130 mM $CsMeSO_4$, 20 mM tetraethylammonium chloride, 1 mM $MgCl_2$, 10 mM EGTA, 10 mM HEPES, 4 mM MgATP, 14 mM Tris-phosphocreatine, 0.3 mM Tris-GTP, 50 units/ml creatine phosphokinase (pH 7.2). In experiments with extracellular application of IGF-1, the perforated patch technique was used to preserve the intracellular milieu of the intact cardiomyocyte. In perforated patch recordings, pipettes were back-filled with 120 mM potassium aspartate, 20 mM KCl, 10 mM NaCl, 2 mM $MgCl_2$, 5 mM HEPES (pH 7.3), supplemented with 240 μg/ml amphotericin-B. Perforated patch recordings were initiated once the access resistance had dropped sufficiently to allow for voltage clamp recordings. Cardiomyocytes were held at −40 mV to inactivate Na^+ currents. Calcium currents were elicited using 300-ms depolarizing voltage steps in increments of 10 mV from −30 to +60 mV. Membrane capacitances were measured using a positive-negative going slow ramp protocol. PClamp software (Molecular Devices) was used for the generation of voltage clamp protocols and data acquisition. Cardiomyocytes were cultured overnight under control conditions or in the presence of As_2O_3 in M199 medium at 37 °C, 5% CO_2. Stock solutions for LY294002, wortmannin, PI3K-γ inhibitor II, Akt inhibitor VIII, SH-6/Akt inhibitor III, and PKC inhibitors bisindolylmaleimide (BisI) and Goe6976 (all from Calbiochem/EMD) were prepared in DMSO and diluted to final concentrations either in M199 medium for overnight incubation or in bath solution for short term incubation. Akt inhibitor VII/TAT-Akt-in (Calbiochem/EMD) and mIGF-1 (Sigma) were prepared directly in bath solution. Stock solutions of the synthetic lipids C8-phospatidylinositol 3,4,5-trisphosphate (C8-PIP_3; C8 indicates short acyl side chains), C8-phospatidylinositol 4,5 bisphosphate (C8-PIP_2), metabolically stabilized C8-PIP_3 3-phosphothioate, and C8-PIP_3 3-methylenephosphonate (all from Echelon Biosciences) were prepared in H_2O, stored at −20 °C, and diluted in intracellular pipette solution just before use. For short term incubations with stabilized C8-PIP_3 3-phosphothioate and C8-PIP_3 3-methylenephosphonate, lipids were directly diluted in extracellular bath solution.

Western Blot Analysis of Oxidized and Reduced Cardiac PTEN—Freshly isolated guinea pig ventricular myocytes were cultured for 4 h at 37 °C in M199 medium under control conditions or in the presence of 10 μM As_2O_3. All solutions used for protein isolations were thoroughly degassed. Following drug treatment, cardiomyocytes were washed in ice-cold PBS and resuspended in a lysis buffer with 20 mM *N*-ethylmaleimide added to block free thiol groups: 0.2% Triton, 50 mM MES (pH 6.5), 100 mM NaCl, 5 mM EDTA, 20 mM *N*-ethylmaleimide, and protease inhibitor mixture (Complete Mini, Roche Applied Science). Protein concentrations were determined by the BCA method (Pierce). PTEN was immunoprecipitated from cardiomyocyte lysates (800–1200 μg) overnight at 4 °C using a goat polyclonal anti-PTEN antibody (20 μl; Santa Cruz Biotechnology, Inc., Santa Cruz, CA). PTEN-antibody complexes were collected for 2 h at 4 °C using protein G beads (Dynal). Bound protein was eluted from protein G beads with citric acid and resolved on non-reducing 10% SDS-PAGE. After transfer to polyvinylidene difluoride membranes, Western blots were developed using a mouse monoclonal anti-PTEN antibody (Santa Cruz Biotechnology, Inc.) followed by incubation with horseradish peroxidase-conjugated secondary antibody (1:3000; 1 h at room temperature; Amersham Biosciences) and ECL Plus (GE Healthcare). Western blots were captured directly on a Kodakimager (GE Healthcare) for quantitative analysis.

Phosphatase Assay of Oxidized and Reduced Forms of Cardiac PTEN—Freshly isolated guinea pig ventricular myocytes were incubated for 4 h at 37 °C in M199 medium under control conditions or in the presence of 10 μM As_2O_3. All solutions used in the assay were thoroughly degassed. To determine oxidized PTEN activity, myocytes were washed in PBS and lysed, protected from light, in a buffer solution containing 1% Triton, 50 mM MES (pH 6.5), 150 mM NaCl, 1 mM EDTA, protease inhibitor mixture (Complete Mini, Roche Applied Science), and 10 mM iodoacetamide. Iodoacetamide was used to irreversibly acetylate free thiol groups, including a cysteine in the active site of PTEN that renders the enzyme non-functional, whereas oxidized active site cysteines are protected. Residual free iodoacetamide was removed from lysates using Zeba Desalt Spin columns (Pierce). Protein concentrations of cleared supernatants were determined by the BCA method (Pierce). PTEN was immunoprecipitated from lysates (about 1 mg) overnight at 4 °C using a rabbit polyclonal anti-PTEN antibody (2 μg of antibody/mg of lysate, Bethyl Laboratories). PTEN-antibody complexes were collected for 2 h at 4 °C on protein G plus agarose. Bound protein-agarose complexes were washed, concentrated by centrifugation, and resuspended in a reducing buffer to recover oxidized cysteines and restore function to previously inactive, oxidized PTEN molecules (100 mM Tris (pH 8), 10 mM DTT). Restored, oxidized PTEN phosphatase activity was measured for 60 min at 37 °C upon the addition of 120 μM C8-PIP_3 (Echelon) to isolated PTEN-agarose complexes. The assay reaction was terminated by a short centrifugation run (5 min, 4 °C) to pellet protein-agarose complexes. Twenty-five microliters of cleared assay

supernatant were quickly removed and added for 15–30 min at room temperature to 100 μl of Malachite Green solution (Echelon) in 96-well format. Release of free phosphate as a function of oxidized PTEN activity was measured as a change in absorbance at 620 nm using a Beckman DTX plate reader. Phosphate standards in the picomolar concentration range were diluted directly in Malachite Green solution to generate a standard curve for quantitative analysis of PTEN activity measurements. To determine total or reduced PTEN activity, cardiomyocytes were lysed directly in a buffer solution (1% Triton, 50 mM MES (pH 6.5), 150 mM NaCl, 1 mM EDTA) supplemented with a 10 mM concentration of the reducing agent DTT to either retain active PTEN cysteines in the reduced, functional state or convert previously oxidized cysteine residues back into the reduced state present in active PTEN. Subsequently, residual DTT was removed from lysates, PTEN was immunoprecipitated, and PTEN phosphatase activity was assayed as described above for measurements of oxidized PTEN activity.

Isoform-specific Measurement of Cardiac Phoshatidylinositol 3-Kinase Activity—Freshly isolated guinea pig cardiomyocytes were incubated for 4 h at 37 °C in M199 under control conditions, in the presence of 10 μM As_2O_3 or of 10 μM As_2O_3, 200 nM wortmannin to inhibit PI3K activity. Myocytes were washed in PBS and lysed in a buffer containing 1% Nonidet P-40, 50 mM Tris (pH 8.0), 150 mM NaCl, 1 mM EDTA, 1 mM EGTA, and protease inhibitor mixture (Roche Applied Science). Lysates were immunoprecipitated using isoform-specific antibodies directed against three different PI3K subunits, p110α, p110β, and p110γ, expressed in the heart (rabbit polyclonal antibodies, Santa Cruz Biotechnology, Inc.). Immunocomplexes were further purified using protein G beads (Dynal) and washed. Isolated immunocomplexes were assayed for PI3K activity while immobilized on protein G beads. The assay reaction was performed for 30 min at 25 °C in buffer containing 20 mM Tris-Cl (pH 7.4), 100 mM NaCl, 10 mM $MgCl_2$, 0.5 mM EGTA, 100 μM L-α-phosphatidylinositol (PI) (Avanti, Alabaster, AL), 20 μM ATP, and 2 μCi of [γ-^{32}P]ATP. The PI3K-catalyzed phosphorylation of PI, producing a radiolabel in the 3-position (phosphatidylinositol 3-phosphate; PI-3P), was terminated by the addition of 1 M HCl. Phospholipids were extracted using a 1:1 chloroform/methanol mixture. After centrifugation, the phospholipid-containing organic phase was isolated from the aqueous phase and dried under a stream of nitrogen gas. After resuspension in a small volume of chloroform/methanol (1:1), lipid samples were spotted on a TLC plate (Analtech, Newark, DE) and resolved using a running buffer system consisting of chloroform/methanol/ammonium hydroxide/water at a volume ratio of 60:47:11.3:2. Radiolabeled PI-3P produced in the assay reaction was quantified directly by analyzing dried TLC plates on a Storm PhosphorImager.

Western Blot Analysis of Akt and Phospho-Akt—Whole cell lysates of guinea pig ventricular myocytes in short term culture were prepared in a lysis buffer containing 0.2% Triton, 50 mM MES (pH 6.5), 100 mM NaCl, 5 mM EDTA, protease inhibitor mixture (Complete Mini, Roche Applied Science), and 20 mM NEM to reduce tyrosine phosphatase activities. Protein concentrations were determined by the BCA method (Pierce). Proteins were separated on reducing SDS-polyacrylamide gels, transferred to polyvinylidene difluoride membranes, and incubated with either a rabbit polyclonal anti-Akt antibody, which detects all three Akt isoforms (Akt1 to -3, Cell Signaling), or a rabbit monoclonal antibody, which detects phospho-Akt (Ser^{473}). Western blots were developed using horseradish peroxidase-conjugated secondary antibody and ECL Plus (GE Healthcare).

Data Analysis—Data are expressed as mean ± S.E. of *n* experiments or cells studied. Differences between means were tested using either a two-tailed Student's *t* test or single factor analysis of variance followed by a two-tailed Dunnett's test to determine whether multiple treatment groups were significantly different from control. *p* values of <0.05 were considered statistically significant.

RESULTS

Therapeutic As_2O_3 Increases Cardiac Calcium Currents—We have previously reported that L-type calcium current amplitudes in guinea pig ventricular myocytes more than double upon overnight exposure to 3 μM As_2O_3 and that amplitude changes follow a fast time course limited only by As_2O_3 gaining access to the cell interior (9). Here we expand on these observations and show that overnight (24-h) exposure to 0.1, 1, and 3 μM As_2O_3, three concentrations that bracket the clinically relevant, therapeutic concentration range of 0.1–1.5 μM (19), increase cardiac calcium currents in a dose-dependent manner (Fig. 1, *A* and *C*). At the same time, current activation was not modified, suggesting that the overall effect is on channel availability (Fig. 1*D*). Importantly, As_2O_3-induced increases in calcium current density could be attenuated by co-incubation with a 10 mM concentration of the antioxidant NAC (Fig. 1, *B* and *E*), similar to what has been described for another redox-active, metalloid compound class (*i.e.* antimony-based anti-leishmanial drugs, such as sodium stibogluconate) (20).

Phosphatidylinositol 3-Kinase Inhibitors Prevent As_2O_3 Effects—We speculated that the redox-sensitive increase in cardiac Ca^{2+} currents observed upon As_2O_3 exposure may be caused via oxidative inactivation of protein-tyrosine phosphatases (PTPs) because antimony and arsenic-based compounds, such as sodium stibogluconate or phenyl arsine oxide, are known potent PTP inhibitors (21–23). Although in the human genome about 100 genes encode for PTPs containing a conserved, redox-sensitive catalytic cysteine residue (24), few PTPs have ever been linked to the modulation of cardiac calcium currents. One exception is PTEN, a structurally related lipid phosphatase that has been linked to a PI3K-dependent increase of cardiac calcium currents in a PTEN$^{-/-}$ mouse model (17). To determine whether PI3K/PTEN signaling may regulate As_2O_3-induced changes in cardiac calcium currents, we investigated the pharmacological effects of two different PI3K inhibitors, LY294002 and wortmannin.

We found in guinea pig ventricular myocytes that co-incubation with LY294002 completely abolished As_2O_3-induced increases in calcium currents (Fig. 2*A*). To address the specificity of this effect, we used wortmannin as an alternative,

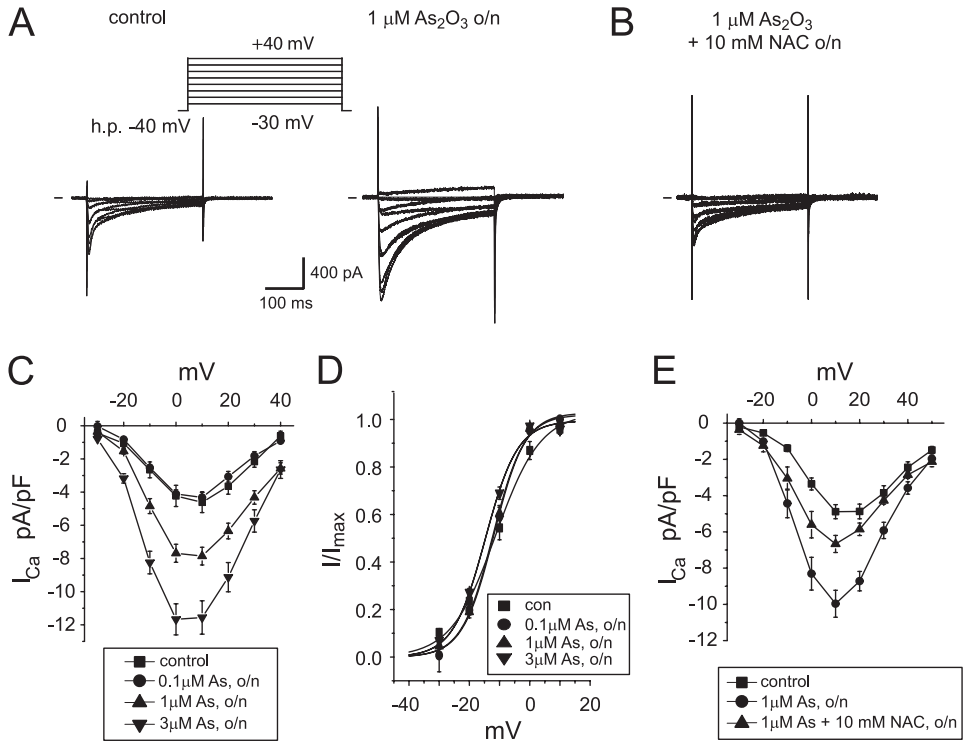

FIGURE 1. **As_2O_3 increases cardiac calcium currents.** *A*, calcium current traces elicited using 300-ms step depolarizations in increments of 10 mV from −30 to +40 mV (h.p. = −40 mV) in guinea pig ventricular myocytes cultured overnight (24 h) under control conditions or in the presence of 1 μM As_2O_3. *h.p.*, holding potential. *B*, typical calcium current traces elicited on co-incubation with 1 μM As_2O_3 and 10 mM NAC. *C*, averaged I-V relationships measured under control conditions and on overnight incubation with 0.1, 1, and 3 μM As_2O_3. At 0 mV, calcium current density was −4.6 ± 0.6 pA/picofarads under control condition, −7.9 ± 0.5 pA/picofarads on overnight incubation with 1 μM As_2O_3, and −11.6 ± 1 pA/picofarads on incubation with 3 μM As_2O_3 (n = 5–15). *D*, steady-state activation of calcium currents measured under control conditions and upon overnight incubation with 0.1, 1, and 3 μM As_2O_3. *E*, averaged I-V relationships measured under control conditions, in the presence of 1 μM As_2O_3, and upon co-incubation with 1 μM As_2O_3, 10 mM NAC (n = 5–8). *o/n*, overnight.

structurally unrelated PI3K inhibitor. Wortmannin is a selective, irreversible inhibitor, albeit with limited stability on long term incubation at 37 °C (25). Therefore, we changed our experimental protocol and co-incubated cardiac myocytes with 3 μM As_2O_3 for 24 h and 100 nM wortmannin for the final 90 min. Similar to experiments with LY294002, As_2O_3 effects were blunted by wortmannin (Fig. 2*B*). Importantly, neither PI3K inhibitor affected cardiac calcium currents under control conditions (Fig. 2*C*). Our data suggest an altered gain in PI3K-dependent signaling pathways, which may be explained best by increased PI3K and/or decreased PTEN activity.

As_2O_3 Does Not Directly Increase Cardiac PI3K Activity—Next, we determined whether direct stimulation of PI3K activity may be responsible for As_2O_3-induced calcium current increases. Guinea pig ventricular myocytes express three different catalytic PI-3K subunits, p110α, -β, and -γ (supplemental Fig. S1). We determined the activity of each subunit under control conditions or after a 4-h incubation with 10 μM As_2O_3. Short term exposure to 10 μM As_2O_3 was sufficient to increase cardiac calcium currents to levels typically achieved upon overnight incubation with 3 μM As_2O_3 and was used to facilitate biochemical analysis (supplemental Fig. S2). In these experiments, we detected primarily p110α/PI3Kα activity under control conditions (Fig. 3, *A* and *B*). However, p110α/PI3K-α activity was not altered by exposure to As_2O_3, whereas it was readily inhibited by wortmannin (Fig. 3, *A* and *B*). In marked contrast, basal activities of both p110β/PI3Kβ and p110γ/PI3Kγ were low either in the absence or presence of As_2O_3 (Fig. 3*B*). To verify the limited contribution of p110γ/PI3Kγ to basal PI3K activity in cardiomyocytes, we performed additional electrophysiological experiments using PI3Kγ inhibitor II, an isoform-specific pharmacological inhibitor of p110γ/PI3Kγ. In line with our biochemical experiments, we found that PI3Kγ inhibitor II did not affect As_2O_3-induced increases in cardiac calcium current amplitudes, not even at very high concentrations of 5 μM (supplemental Fig. S3).

Finally, we tested for the functional integrity of PI3Kα signaling using IGF-1, which enhances cardiac calcium currents in mouse hearts via a PI3-Kα/Akt dependent pathway (17). We found that calcium currents were increased within 5 min by about 35%, when guinea pig cardiomyoctes were acutely perfused with 100 ng/ml IGF-1. IGF-1 effects could be blocked with 100 nM wortmannin (supplemental Fig. S4). Overall, however, IGF-1 effects were modest compared with the large increase in current amplitude seen on incubation with As_2O_3.

Oxidative Inactivation of the Lipid Phosphate PTEN by As_2O_3—Because our data suggest that PI3Ks were not a direct target for As_2O_3, we tested whether exposure of cardiomyocytes to As_2O_3 may instead result in the oxidative inactivation of PTEN, a downstream lipid phosphatase that antagonizes PI3K signaling. PTEN is known to be readily oxidized and inactivated by exposure to H_2O_2 or as a consequence of growth factor signaling (26–29). Upon oxidation, PTEN can be detected directly by non-reducing SDS-PAGE because it

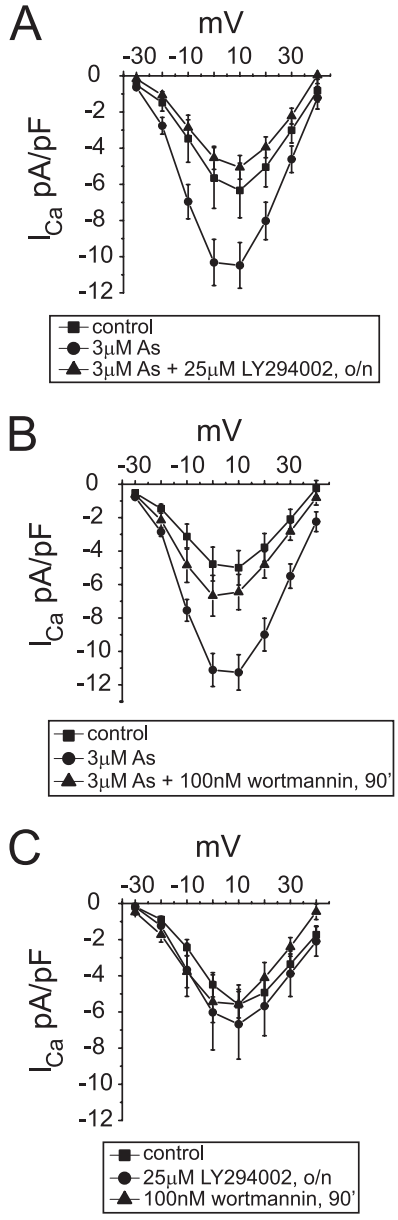

FIGURE 2. **As_2O_3-induced increases in cardiac calcium currents are abolished by PI3K inhibitors.** Calcium current traces were elicited as described in the legend to Fig. 1. *A*, averaged I-V relationships showing current densities measured under control conditions, upon overnight (*o/n*) incubation with 3 μM As_2O_3, and upon co-incubation with 3 μM As_2O_3 + 25 μM LY294002 overnight; *B*, averaged I-V relationships measured under control conditions, upon overnight incubation with 3 μM As_2O_3, and following a 90-min incubation with 100 nM wortmannin after overnight exposure to 3 μM As_2O_3; *C*, neither LY294002 (overnight) nor wortmannin (90 min) affects control calcium currents (n = 5–15). Data are expressed as mean ± S.E.

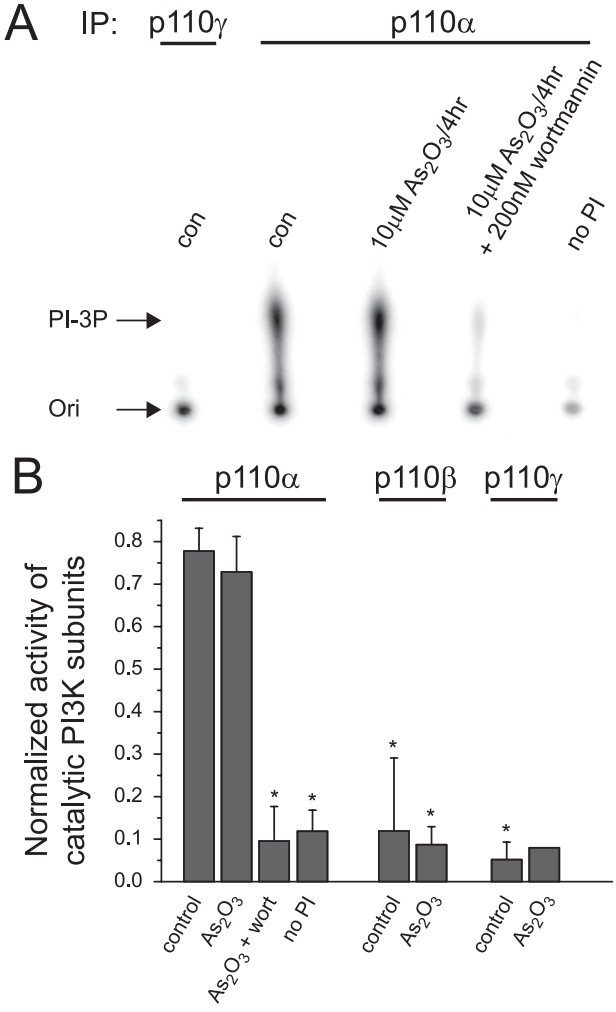

FIGURE 3. **As_2O_3 does not increase cardiac PI3K activity.** Freshly isolated guinea pig ventricular myocytes were incubated for 4 h under control conditions or in the presence of 10 μM As_2O_3. Catalytic PI3K subunits p110α, p110β, and p110γ were immunoprecipitated from whole cell lysates. PI3K activity of immunocomplexes was assayed as a function of PI-3P production. *A*, shown is a typical autoradiogram of ^{32}P-labeled PI-3P produced on immunoprecipitation (*IP*) of p110γ or p100α and resolved by TLC. *Ori*, origin of TLC migration. Incubation with As_2O_3 does not alter PI-3P production, whereas co-incubation with 200 nM wortmannin inhibits PI-3P production. PI-3P production is not observed upon the omission of substrate from the assay reaction (*no PI*). Note that the basal activity of PI3K-γ/p110γ is very low under control conditions. *B*, quantitative analysis of PI3K/p110 activities. Shown is normalized PI-3P production under control conditions or in the presence of 10 μM As_2O_3 for PI-3K/p110α, -β, and -γ. PI-3K/p110α activity is significantly inhibited by 200 nM wortmannin. Assays without the addition of PI were used as negative controls (n = 1–5). *, significant difference from PI-3K/p100α activity measured under control conditions (Dunnett's test, $p < 0.05$). *Error bars*, S.E.

migrates faster than the reduced form of PTEN. To test for As_2O_3-induced oxidation, we exposed freshly isolated guinea pig ventricular myocytes for 4 h to 10 μM As_2O_3 or a combination of 10 μM As_2O_3 with 10 mM NAC. Because expression is low in cardiomyocytes, PTEN was immunoprecipitated from whole cell lysates prior to detection by non-reducing SDS-PAGE. On Western blots, we found that exposure to As_2O_3 produced a fast migrating, oxidized form of PTEN (Fig. 4*A*). Under our experimental conditions, about 30% of PTEN was oxidized upon exposure to 10 μM As_2O_3 (Fig. 4*B*). In addition, PTEN oxidation could be prevented by co-incubation with 10 mM NAC (Fig. 4, *A* and *B*).

We independently verified our results by determining the activity of PTEN using a specific phosphatase assay. To measure the activity of PTEN that has been oxidized in cardiomyocytes upon exposure to As_2O_3, we prepared whole cell lysates in the presence of iodoacetamide to acetylate all available free thiol groups, including a catalytic cysteine residue in the active site of PTEN, whereas oxidized cysteine residues were protected. We then used the reducing agent DTT to recover oxidized cysteine residues, thereby restoring function to pre-

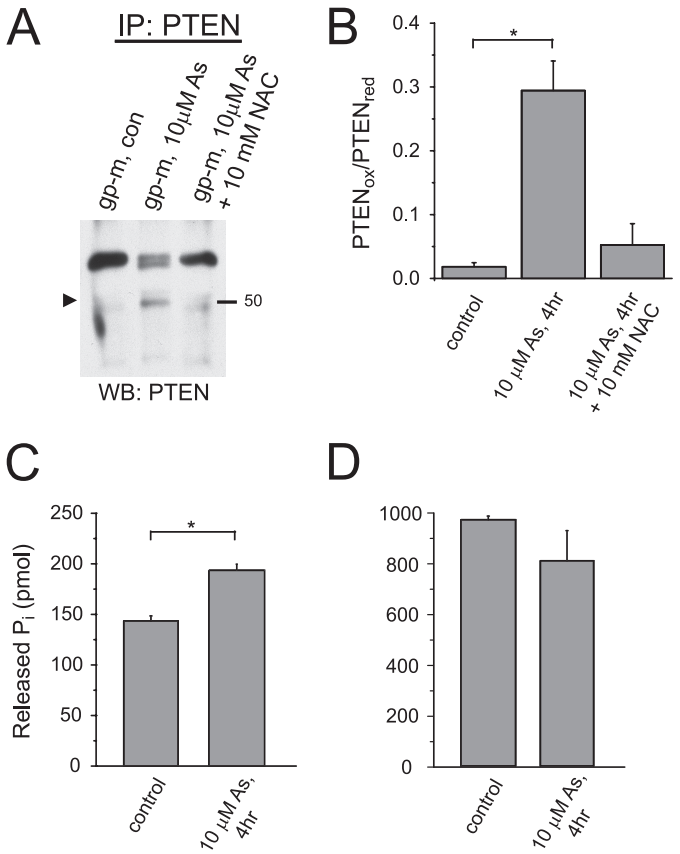

FIGURE 4. *A*, Western blot showing PTEN expressed under control conditions (*con*) in guinea pig ventricular myocytes (*gp-m*) and following incubation with 10 μM As_2O_3 for 4 h. Co-incubation of 10 μM As_2O_3 together with 10 mM NAC prevented oxidation of PTEN. PTEN was immunoprecipitated from whole cell lysates prior to detection on non-reducing SDS-PAGE. *Arrowhead*, position of oxidized PTEN. *B*, quantitative analysis of PTEN oxidation in cardiomyocytes on exposure to As_2O_3 ($n = 3–4$). As_2O_3 increases the oxidized form of PTEN significantly (Dunnett's test, $p < 0.05$). *C*, detection of oxidized PTEN by phosphatase assay. Cardiomyocytes were incubated for 4 h either under control conditions or in the presence of 10 μM As_2O_3 and lysed in the presence of iodoacetamide. PTEN was immunoprecipitated and assayed for phosphatase activity under reducing conditions. Measurements are expressed as the amount of phosphate released from PIP_3 by PTEN. Note, that phosphate release is different between control- and As_2O_3-treated myocytes at the $p < 0.05$ level. *D*, detection of total PTEN activity by phosphatase assay. Cardiomyocytes were incubated for 4 h either under control conditions or in the presence of 10 μM As_2O_3 and lysed under reducing conditions. Importantly, total phosphate release was not different between control and As_2O_3-treated myocytes. *IP*, immunoprecipitation; *WB*, Western blot. *Error bars*, S.E.

viously inactive PTEN. Restored, oxidized PTEN activity was monitored as a function of phosphate released from soluble C8-PIP_3 added to the assay reaction (Fig. 4*C*). In these experiments, we reproducibly detected a fraction of PTEN that became oxidized in the presence of As_2O_3, similar to results obtained from immunoblots.

In addition, we determined total PTEN activity in control cardiomyocytes as well as in myocytes exposed to 10 μM As_2O_3. In these experiments, lysates were prepared directly in a reducing buffer either to retain PTEN in a functional state or to return oxidized PTEN back into the functional state. We found that total PTEN activity was not different between As_2O_3-treated and control myocytes (Fig. 4*D*). This suggests that under our experimental conditions, As_2O_3 exposure did not change PTEN expression but produced PTEN molecules that had been inactivated via oxidation.

Oxidative Inactivation of PTEN Regulates Akt Activity—Following oxidative inactivation of PTEN, we expected PIP_3 levels to rise, given the high basal PI3Kα activity measured in cardiomyocytes. Because direct quantitation of PIP_3 levels was not feasible given the relatively small number of isolated cardiomyocytes available in individual experiments, we used Akt phosphorylation as a surrogate marker. As a direct consequence of an increase in PIP_3 levels, the downstream target Akt should be recruited to the plasma membrane via interaction between its pleckstrin domain and PIP_3. PIP_3-induced translocation and subsequent activation of Akt can be monitored directly by assessing phosphorylation of Akt residues Thr^{308} or Ser^{473} (30). To test whether Akt was activated as predicted, we performed Western blots to determine Akt phosphorylation in cardiac myocytes under control conditions or upon exposure to As_2O_3. We found that phosphorylation of Akt Ser^{473} increased (*i.e.* that Akt was activated) when cardiomyocytes were exposed to 10 μM As_2O_3. At the same time, the As_2O_3-induced increase in Akt phosphorylation could be blocked using Akt inhibitor VIII (Fig. 5*A*). Because Akt activation had previously been linked to an increase of cardiac L-type calcium currents (*e.g.* in $PTEN^{-/-}$ mice), we investigated whether a set of pharmacological inhibitors of Akt may similarly abrogate As_2O_3-induced L-type calcium current changes in guinea pig ventricular myocytes. We used three structurally different, pharmacological inhibitors of Akt, Akt inhibitor VIII at 5 μM, SH-6 (Akt inhibitor III) at 10 μM, and TAT-Akt-in (Akt inhibitor VII, a peptide inhibitor) at 30 μM either overnight in combination with As_2O_3 or for 90 min in myocytes pretreated with As_2O_3 (Fig. 5, *B–D*). Surprisingly, none of these inhibitors affected As_2O_3-induced calcium current increases, indicating that As_2O_3 may regulate L-type calcium currents by another pathway downstream of PTEN.

Because Akt inhibition was ineffective, we pursued protein kinase C (PKC) as an alternative target, because skeletal muscle L-type calcium currents are activated by IGF-1 via PKC-dependent pathways (31). Similarly, in myocytes isolated from rabbit portal vein, PI3K-dependent stimulation of L-type calcium currents requires downstream PKC activity (32). Consequently, we tested two PKC inhibitors for their ability to modulate As_2O_3-dependent increases in L-type calcium currents. We used BisI as a broad spectrum PKC inhibitor and Goe6976 as an inhibitor targeting preferentially classic, Ca^{2+}-dependent PKC isoforms. In these experiments, we found that both 30 and 300 nM Goe6976 reduced increases in calcium current densities (Fig. 6, *A* and *B*), whereas 300 nM BisI inhibited As_2O_3-dependent current increases completely (Fig. 6*C*). Although these results suggest that classic PKC isoforms are at least partially involved in As_2O_3-initiated signaling events, calcium currents could not be stimulated in guinea pig ventricular myocytes with the phorbol ester phorbol 12,13-dibutyrate (at 200 nM) applied to activate classic PKC isoforms (supplemental Fig. S5). Because the magnitude of As_2O_3-induced amplitude changes rivaled those seen on activation of cAMP/PKA signaling, we also tested whether current increases may be blunted via PKA inhibition. However, in

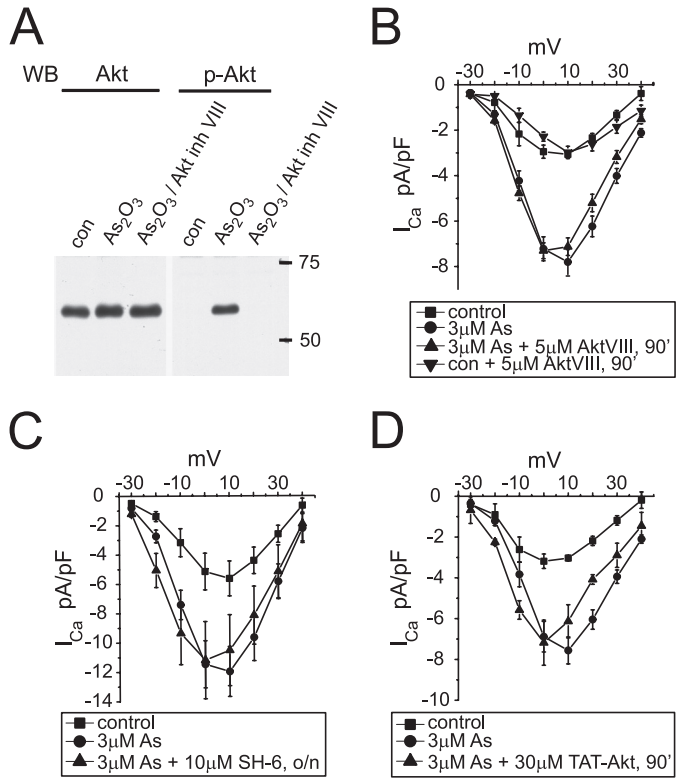

FIGURE 5. **As_2O_3-induced calcium current increases are not blocked by Akt inhibitors.** *A*, Western blot (*WB*) of whole cell lysates showing total Akt and phospho-Akt Ser^{473} (*p-Akt*) in guinea pig ventricular myocytes under control conditions (*con*), following incubation with 10 μM As_2O_3 for 4 h, and following co-incubation with 10 μM As_2O_3 and 5 μM Akt inhibitor VIII for 4 h. Note that As_2O_3 exposure initiates Akt phosphorylation/activation, which can be completely blocked by Akt inhibitor VIII. *B*, cardiac calcium current traces in *B–D* were elicited in guinea pig ventricular myocytes as described in Fig. 1. Averaged I-V relationships show that 5 μM Akt inhibitor VIII does not inhibit As_2O_3-induced calcium current increases. AktVIII was applied for 90 min upon overnight incubation of cardiomyocytes with 3 μM As_2O_3. Note that control currents are not affected by AktVIII. *C*, averaged I-V relationships showing that 10 μM SH-6 does not inhibit As_2O_3-induced calcium current increases. Cardiomyocytes were co-incubated overnight with both 10 μM SH-6 and 10 μM As_2O_3. *D*, a 30 μM concentration of the inhibitory peptide TAT-AktVII does not affect As_2O_3-induced calcium current increases. The inhibitory peptide was applied with the extracellular perfusate for 90 min upon overnight incubation of cardiomyocytes with 3 μM As_2O_3 ($n = 5–8$). *Error bars*, S.E.

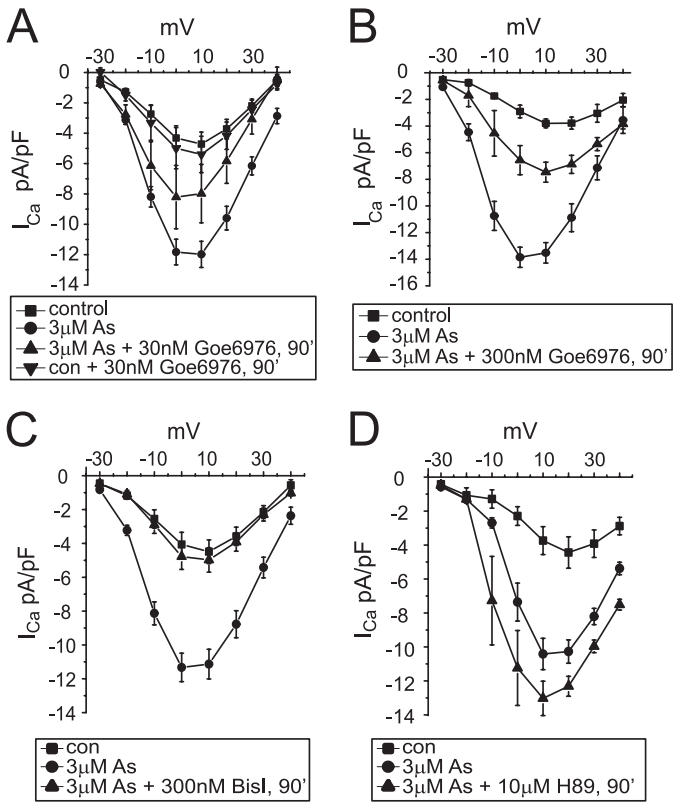

FIGURE 6. **As_2O_3-induced increases in cardiac calcium currents are blocked by PKC inhibitors.** Calcium current traces were elicited in guinea pig ventricular myocytes as described in the legend to Fig. 1. *A*, averaged I-V relationships showing partial inhibition of As_2O_3-induced calcium current increases by 30 nM Goe6976. Goe6976 was applied for 90 min following overnight incubation of cardiomyocytes with 3 μM As_2O_3. Note that control currents are not affected by 30 nM Goe6976. *B*, averaged I-V relationships showing inhibition of As_2O_3-induced calcium current increases by 300 nM Goe6976 applied for 90 min. *C*, averaged I-V relationships showing complete inhibition of As_2O_3-induced calcium current increases by 300 nM BisI applied for 90 min ($n = 5–23$). *D*, As_2O_3-induced calcium current increases are not attenuated by incubation with a 10 μM concentration of the PKA inhibitor H89 applied for 90 min; averaged I-V relationships ($n = 5$). *Error bars*, S.E.

marked contrast to our experiments with PKC inhibitors, we found that incubation with a 10 μM concentration of the specific PKA inhibitor H89 did not reduce L-type calcium current increases upon As_2O_3 exposure (Fig. 6*D*).

PIP_3 Increases Calcium Currents in Cardiomyocytes Pretreated with Submaximal As_2O_3 Concentrations—Because our results suggest that an Akt-independent pathway is involved that relies on PIP_3 as a trigger, we tested whether PIP_3 may directly modulate L-type calcium currents. In these experiments, we first perfused freshly isolated guinea pig ventricular myocytes with increasing concentrations of C8-PIP_3 via the patch pipette and measured maximal calcium current amplitudes immediately and 5 min after gaining whole cell access. We found that intracellular application of C8-PIP_3 had no effect on calcium current amplitudes (Fig. 7*A*). Because PIP_3 effects may be compromised by inadequate compound stability, we repeated our internal perfusion experiments with two additional lipid compounds in which the 3-phosphate bond of PIP_3 has been metabolically stabilized. In addition, we incubated cardiomyocytes for 1 h in the presence of a 25 μM concentration of metabolically stabilized C8-PIP_3 derivatives before current recordings were started. Again, calcium current densities were not significantly affected by either internal or external PIP_3 application (Fig. 7*B* and supplemental Fig. S6*A*). Similarly, calcium current amplitudes were not increased by incubation with bisperoxo (bipyridine) oxovanadate, a potent chemical phosphatase inhibitor that is thought to block PTEN with some specificity ($IC_{50} = 18$ nM; Fig. 7*C*) (33). To explore whether PIP_3 may synergize with additional As_2O_3-induced oxidation events, we pretreated cardiomyocytes overnight with a submaximal As_2O_3 concentration (1 μM), which by itself increases calcium current density only modestly (see Fig. 1). Pretreated cardiomyocytes were then perfused with 1 μM either C8-PIP_3 or C8-PIP_2 via the patch pipette. Under these conditions, internal application of 1 μM PIP_3 more than doubled calcium current densities within 5 min, whereas internally applied PIP_2 was without any effect (Fig. 7, *D* and *E*, and supplemental Fig. S6*B*). Taken together, our data suggest that elevated PIP_3 levels are necessary but

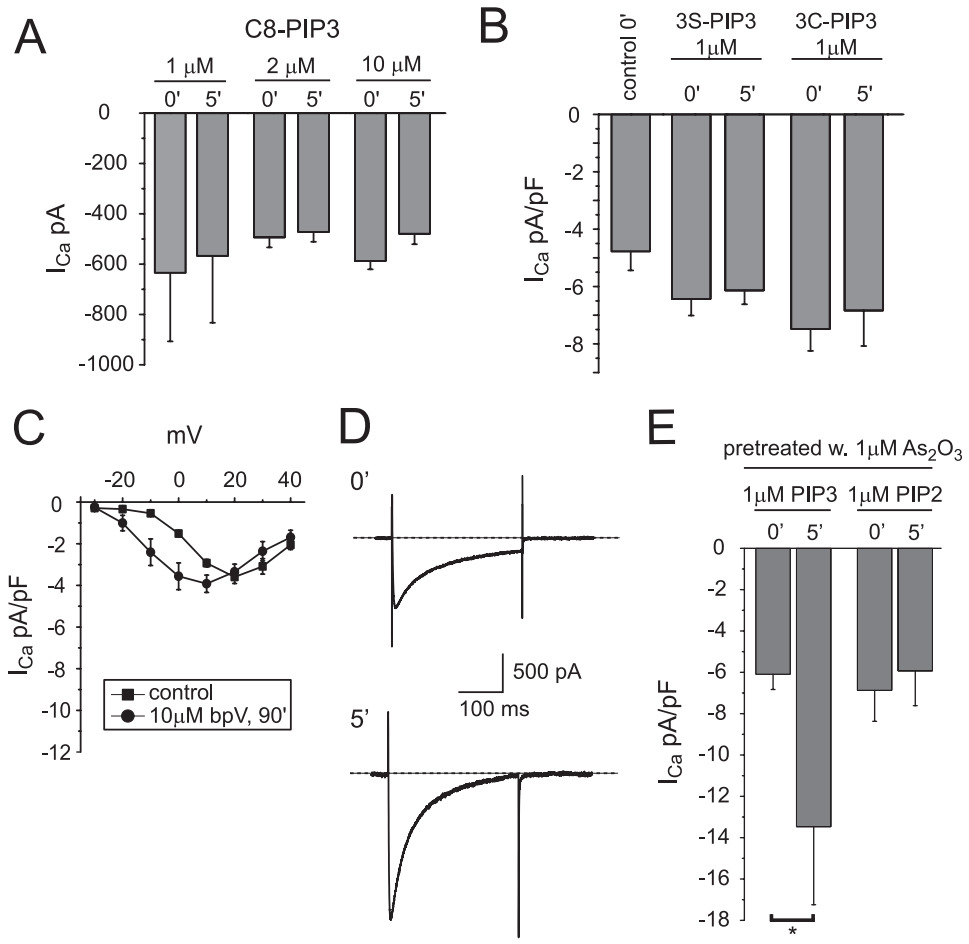

FIGURE 7. **Changes in calcium current density on internal perfusion with PIP_3.** *A*, maximal calcium current amplitudes measured in guinea pig ventricular myocytes on internal perfusion with 1, 2, or 10 μM C8-PIP_3 immediately (*0'*) and 5 min (*5'*) after gaining whole cell access ($n = 3–4$). *B*, maximal calcium current densities measured in cardiomyocytes on internal perfusion with a 1 μM concentration of the metabolically stabilized PIP_3 derivative C8-PIP3 (*3S-PIP3*) or C8-PIP3 3-methylenephosphonate (*3C-PIP3*) immediately and 5 min after gaining whole cell access ($n = 5–6$). *C*, averaged I-V relationships measured under control conditions or following a 90-min incubation with a 10 μM concentration of the phosphatase inhibitor bpV. *D*, calcium current traces elicited in a cardiomyocyte with a depolarizing test pulse to +20 mV from a holding potential of −40 mV immediately and 5 min after the start of internal perfusion with 1 μM C8-PIP_3. Calcium currents were recorded following overnight incubation with 1 μM As_2O_3. *E*, maximal current densities measured in cardiomyocytes on internal perfusion with 1 μM either PIP_3 or PIP_2 following overnight incubation with 1 μM As_2O_3 immediately and 5 min after gaining whole cell access ($n = 5$). Note that internal application of C8-PIP_3 increases calcium current density significantly at the $p < 0.05$ level. *Error bars*, S.E.

not sufficient to increase L-type calcium current densities in guinea pig ventricular myocytes. More importantly, As_2O_3 may modify a secondary target downstream of PTEN that has yet to be identified, sensitizing it to modulation by PIP_3.

DISCUSSION

We have analyzed the molecular mechanisms underlying the proarrhythmic modification of cardiac L-type calcium currents by As_2O_3 and found that oxidative inactivation of the lipid phosphatase PTEN represents the primary mechanism. In our experiments, we have detected an inactive, oxidized form of PTEN directly on Western blots as well as indirectly in an enzymatic assay. Furthermore, oxidation of PTEN was blunted in biochemical experiments by co-incubation with the anti-oxidant NAC, which at the same time reduced As_2O_3 effects in electrophysiological experiments. As a member of the cysteine-based PTP superfamily, PTEN has long been recognized as a sensitive target for oxidative inactivation by H_2O_2, either directly or indirectly following exposure of target cells to growth factors that are thought to generate reactive oxygen species and H_2O_2 via activation of NADPH oxidases (24, 26–29). Because As_2O_3 exposure has been shown to generate reactive oxygen species and produce oxidative stress in cardiomyocytes as well as in various other cell types (34, 35), we attribute the As_2O_3-induced inactivation of cardiac PTEN at the structural level to the well characterized oxidative formation of a disulfide bridge between Cys-71 and Cys-124 in the active site of the enzyme (36). It is noteworthy that we were not able to detect sulfenation of PTEN in intact cardiomyocytes because sulfenic acids represent the principle reaction product between cysteine residues and reactive oxygen species/H_2O_2. One explanation may be that sulfenic acids are highly unstable, short lived intermediates that are very rapidly converted into disulfides in the presence of a neighboring cysteine. Consequently, sulfenic acid-modified PTEN may be present only in minute quantities that may be hard to capture.

Besides being exquisitely sensitive to oxidation, PTEN is unique in that it nearly exclusively regulates PI3K signaling at

the plasma membrane. Consequently, cells that lack PTEN show elevated PIP_3 levels and activated Akt-dependent signaling (30). The unique role played by PTEN was reflected in our experiments, with As_2O_3 effects being abolished upon pharmacological inhibition of PI3Ks. Furthermore, Akt-dependent signaling was activated. At the same time, As_2O_3-induced inactivation of PTEN mirrored changes observed in a genetic mouse model with muscle-specific ablation of PTEN ($PTEN^{-/-}$) (17). For example, loss of PTEN in mouse cardiomyocytes was accompanied by a modest increase in L-type calcium current density, whereas pharmacological block of PI3K signaling reduced L-type calcium current densities in $PTEN^{-/-}$ cardiomyocytes to "wild type" levels. Furthermore, cardiac calcium currents in wild type animals were not affected by PI3K inhibition, similar to what we have described under control conditions in guinea pig ventricular myocytes. Finally, elevated L-type calcium current densities were completely reversed in $PTEN^{-/-}$ mice on simultaneous expression of a dominant negative PI3Kα transgene, which matches our observation that basal activity of PI3Kα was high in guinea pig ventricular myocytes, whereas both PI3Kβ and -γ activities are low.

Despite all similarities, we have discovered one major difference. Importantly, in $PTEN^{-/-}$ as well as in $PDK1^{-/-}$ knock-out models, modulation of L-type cardiac calcium currents is strictly dependent on Akt activation (17, 37) (*i.e.* any increase in current levels is reversed on pharmacological inhibition of Akt). Clearly, Akt is the best characterized target for PI3K-derived PIP_3 (30). This can also be seen in transgenic mice overexpressing "active" Akt, which have increased cardiac calcium current levels (38). However, Akt does not appear to be crucial for modulation of L-type calcium channels in As_2O_3-exposed guinea pig cardiomyocytes. Given our extensive efforts, we suggest that PIP_3 may utilize an alternative signaling pathway that most likely diverges at the level of PDK1 immediately upstream of Akt. This is not without precedent, because PDK1 is known to activate several other substrates in addition to Akt, including different PKC isoforms, p70-S6K kinases, p90-RSK kinases, SGK kinases, and even PKA (39). In fact, PI3K-dependent stimulation of calcium currents has been linked to PKC activation in both skeletal and smooth muscle myocytes (31, 32). Similarly, we found that As_2O_3 effects were blunted by PKC inhibitors. At the same time, identification of a specific PKC isoform underlying As_2O_3 effects was complicated by the fact that at least three classic (α, βII, and γ), one novel (ϵ), and one atypical (ξ) isoform are thought to be expressed in guinea pig heart (40). Thus, it will be necessary in the future to follow-up on pharmacological experiments with biochemical assays to determine exactly which PKC isoform may signal toward L-type calcium channels in guinea pig ventricular myocytes.

Furthermore, we have infused guinea pig cardiomyocytes with PIP_3 or metabolically stabilized variants thereof under the assumption that the proposed, Akt-independent pathway may rely on PIP_3 as a trigger (39). Quite unexpectedly, intracellularly applied PIP_3 did not increase cardiac L-type calcium currents, similar to what has been described for mouse cardiomyocytes (41). This excludes the possibility that PIP_3 may

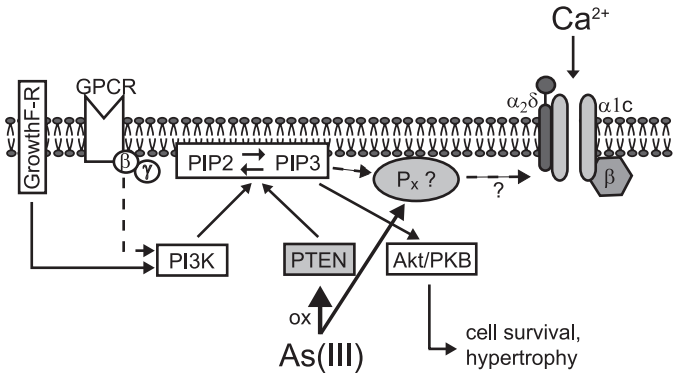

FIGURE 8. **Diagram of the proposed As_2O_3-modified signaling pathways.** For a detailed description, see "Discussion."

directly modulate the calcium channel complex, as shown for ENaC or TRP channels (42, 43). In marked contrast, following preincubation with submaximal As_2O_3 concentrations, guinea pig cardiomyocytes responded with a rapid increase of L-type calcium current levels upon infusion of PIP_3 but not PIP_2. Based on these data and additional experiments with the phosphatase inhibitor bpV, we conclude that an increase in PIP_3 levels is necessary but not sufficient to initiate the As_2O_3-dependent increase in L-type calcium currents. We propose that As_2O_3 modifies an additional, secondary target downstream of PTEN. This downstream leg of the signaling pathway may not be required under basal conditions but may become unmasked upon exposure to oxidative stress.

Overall, the following signaling scheme emerges for the fast activation of cardiac L-type calcium currents by As_2O_3 in guinea pig ventricular myocytes (Fig. 8). Under control conditions basal activity of PI3Kα is high with its PIP_3 output being degraded completely by PTEN. Thus, cellular PIP_3 levels remain low and neither activate downstream Akt nor increase cardiac L-type calcium currents. This may explain why calcium current density is not affected by pharmacological PI3K blockade under control conditions. Here it is important that basal PIP_3 production is dependent on a delicate balance between actual PI3K and PTEN activities, which may vary between cardiomyocytes isolated from different species or mouse strains (see supplemtnal Fig. S7). Following exposure to As_2O_3, cardiac PTEN is oxidized and inactivated, which alters the balance between PIP_3 production and PTEN-mediated degradation. In guinea pig ventricular myocytes, even a modest reduction in PTEN activity seems to be sufficient to increase cellular PIP_3 levels, as shown by robust Akt activation. We propose that PIP_3 signaling diverges downstream of PTEN and activates L-type calcium currents independently of Akt along a pathway that includes a secondary oxidation-sensitive target. The molecular nature of this secondary target as well as its interaction with PIP_3 or calcium channels for that matter is currently unknown and has to be elucidated in future experiments.

Taken together, our study identifies chemical inactivation of the signaling enzyme PTEN as the primary mechanism underlying fast As_2O_3-induced modulation of cardiac L-type calcium currents, thereby strengthening the notion that concerted modification of two major cardiac membrane currents,

hERG/I_{Kr} and L-type calcium currents, may be responsible for the extremely high incidence of torsades de pointes arrhythmias observed in patients treated with As_2O_3 (5, 6). The proposed mechanism may also help us understand why occasionally arrhythmias have been reported within a few h of As_2O_3 application, which could not be easily explained with "slow" hERG trafficking inhibition (19). Furthermore, our study raises the important question of whether there is need for cardiological long term follow-up in patients treated with As_2O_3 because we show here that As_2O_3 modifies PI3K-dependent signaling pathways that are also used in pathophysiological settings of cardiac stress and growth regulation. Most importantly, however, our study introduces a novel mechanistic concept for acLQTS that is centered on the drug-induced modulation of an intracellular signaling cascade. The mechanism outlined may also deepen our understanding of acLQTS precipitated by antimony-based anti-leishmania drugs, such as sodium stibogluconate, that are redox-active just like arsenic. This may explain similarities in the cardiotoxic profile observed with both compound classes, including a fast increase in cardiac L-type calcium currents (20). In addition, our study may focus attention toward other anti-cancer compounds that act, at least in part, via induction of reactive oxygen or nitrogen species. Examples are nitric oxide-donating aspirin, phosphoaspirin, phosphosulindac, and platinium-based anti-cancer compounds, such as cisplatin and its derivatives (44, 45).

REFERENCES

1. Shen, Z. X., Shi, Z. Z., Fang, J., Gu, B. W., Li, J. M., Zhu, Y. M., Shi, J. Y., Zheng, P. Z., Yan, H., Liu, Y. F., Chen, Y., Shen, Y., Wu, W., Tang, W., Waxman, S., De Thé, H., Wang, Z. Y., Chen, S. J., and Chen, Z. (2004) *Proc. Natl. Acad. Sci. U.S.A.* **101,** 5328–5335
2. Nasr, R., Guillemin, M. C., Ferhi, O., Soilihi, H., Peres, L., Berthier, C., Rousselot, P., Robledo-Sarmiento, M., Lallemand-Breitenbach, V., Gourmel, B., Vitoux, D., Pandolfi, P. P., Rochette-Egly, C., Zhu, J., and de Thé, H. (2008) *Nat. Med.* **14,** 1333–1342
3. Wang, Z. Y., and Chen, Z. (2008) *Blood* **111,** 2505–2515
4. Platanias, L. C. (2009) *J. Biol. Chem.* **284,** 18583–18587
5. Ohnishi, K., Yoshida, H., Shigeno, K., Nakamura, S., Fujisawa, S., Naito, K., Shinjo, K., Fujita, Y., Matsui, H., Takeshita, A., Sugiyama, S., Satoh, H., Terada, H., and Ohno, R. (2000) *Ann. Intern. Med.* **133,** 881–885
6. Unnikrishnan, D., Dutcher, J. P., Varshneya, N., Lucariello, R., Api, M., Garl, S., Wiernik, P. H., and Chiaramida, S. (2001) *Blood* **97,** 1514–1516
7. Chiang, C. E., Luk, H. N., Wang, T. M., and Ding, P. Y. (2002) *Blood* **100,** 2249–2252
8. Sanguinetti, M. C., and Tristani-Firouzi, M. (2006) *Nature* **440,** 463–469
9. Ficker, E., Kuryshev, Y. A., Dennis, A. T., Obejero-Paz, C., Wang, L., Hawryluk, P., Wible, B. A., and Brown, A. M. (2004) *Mol. Pharmacol.* **66,** 33–44
10. Splawski, I., Timothy, K. W., Decher, N., Kumar, P., Sachse, F. B., Beggs, A. H., Sanguinetti, M. C., and Keating, M. T. (2005) *Proc. Natl. Acad. Sci. U.S.A.* **102,** 8089–8096
11. Xie, L. H., Chen, F., Karagueuzian, H. S., and Weiss, J. N. (2009) *Circ. Res.* **104,** 79–86
12. Kumagai, Y., and Sumi, D. (2007) *Annu. Rev. Pharmacol. Toxicol.* **47,** 243–262
13. Sulis, M. L., and Parsons, R. (2003) *Trends Cell Biol.* **13,** 478–483
14. Le Blanc, C., Mironneau, C., Barbot, C., Henaff, M., Bondeva, T., Wetzker, R., and Macrez, N. (2004) *Circ. Res.* **95,** 300–307
15. Blair, L. A., and Marshall, J. (1997) *Neuron* **19,** 421–429
16. Viard, P., Butcher, A. J., Halet, G., Davies, A., Nürnberg, B., Heblich, F., and Dolphin, A. C. (2004) *Nat. Neurosci.* **7,** 939–946
17. Sun, H., Kerfant, B. G., Zhao, D., Trivieri, M. G., Oudit, G. Y., Penninger, J. M., and Backx, P. H. (2006) *Circ. Res.* **98,** 1390–1397
18. Ficker, E., Dennis, A. T., Wang, L., and Brown, A. M. (2003) *Circ. Res.* **92,** e87–e100
19. Siu, C. W., Au, W. Y., Yung, C., Kumana, C. R., Lau, C. P., Kwong, Y. L., and Tse, H. F. (2006) *Blood* **108,** 103–106
20. Kuryshev, Y. A., Wang, L., Wible, B. A., Wan, X., and Ficker, E. (2006) *Mol. Pharmacol.* **69,** 1216–1225
21. Pathak, M. K., and Yi, T. (2001) *J. Immunol.* **169,** 3391–3397
22. Garcia-Morales, P., Minami, Y., Luong, E., Klausner, R. D., and Samelson, L. E. (1990) *Proc. Natl. Acad. Sci. U.S.A.* **87,** 9255–9259
23. Hecht, D., and Zick, Y. (1992) *Biochem. Biophys. Res. Commun.* **188,** 773–779
24. Alonso, A., Sasin, J., Bottini, N., Friedberg, I., Friedberg, I., Osterman, A., Godzik, A., Hunter, T., Dixon, J., and Mustelin, T. (2004) *Cell* **117,** 699–711
25. Holleran, J. L., Egorin, M. J., Zuhowski, E. G., Parise, R. A., Musser, S. M., and Pan, S. S. (2003) *Anal. Biochem.* **323,** 19–25
26. Lee, S. R., Yang, K. S., Kwon, J., Lee, C., Jeong, W., and Rhee, S. G. (2002) *J. Biol. Chem.* **277,** 20336–20342
27. Leslie, N. R., Bennett, D., Lindsay, Y. E., Stewart, H., Gray, A., and Downes, C. P. (2003) *EMBO J.* **22,** 5501–5510
28. Kwon, J., Lee, S. R., Yang, K. S., Ahn, Y., Kim, Y. J., Stadtman, E. R., and Rhee, S. G. (2004) *Proc. Natl. Acad. Sci. U.S.A.* **101,** 16419–16424
29. Seo, J. H., Ahn, Y., Lee, S. R., Yeol Yeo, C., and Chung Hur, K. (2005) *Mol. Biol. Cell* **16,** 348–357
30. Oudit, G. Y., and Penninger, J. M. (2009) *Cardiovasc. Res.* **82,** 250–260
31. Delbono, O., Renganathan, M., and Messi, M. L. (1997) *J. Neurosci.* **17,** 6918–6928
32. Callaghan, B., Koh, S. D., and Keef, K. D. (2004) *Circ. Res.* **94,** 626–633
33. Schmid, A. C., Byrne, R. D., Vilar, R., and Woscholski, R. (2004) *FEBS Lett.* **566,** 35–38
34. Liu, S. X., Athar, M., Lippai, I., Waldren, C., and Hei, T. K. (2001) *Proc. Natl. Acad. Sci. U.S.A.* **98,** 1643–1648
35. Chou, W. C., Jie, C., Kenedy, A. A., Jones, R. J., Trush, M. A., and Dang, C. V. (2004) *Proc. Natl. Acad. Sci. U.S.A.* **101,** 4578–4583
36. Lee, J. O., Yang, H., Georgescu, M. M., Di Cristofano, A., Maehama, T., Shi, Y., Dixon, J. E., Pandolfi, P., and Pavletich, N. P. (1999) *Cell* **99,** 323–334
37. Catalucci, D., Zhang, D. H., DeSantiago, J., Aimond, F., Barbara, G., Chemin, J., Bonci, D., Picht, E., Rusconi, F., Dalton, N. D., Peterson, K. L., Richard, S., Bers, D. M., Brown, J. H., and Condorelli, G. (2009) *J. Cell Biol.* **184,** 923–933
38. Kim, Y. K., Kim, S. J., Yatani, A., Huang, Y., Castelli, G., Vatner, D. E., Liu, J., Zhang, Q., Diaz, G., Zieba, R., Thaisz, J., Drusco, A., Croce, C., Sadoshima, J., Condorelli, G., and Vatner, S. F. (2003) *J. Biol. Chem.* **278,** 47622–47628
39. Vasudevan, K. M., Barbie, D. A., Davies, M. A., Rabinovsky, R., McNear, C. J., Kim, J. J., Hennessy, B. T., Tseng, H., Pochanard, P., Kim, S. Y., Dunn, I. F., Schinzel, A. C., Sandy, P., Hoersch, S., Sheng, Q., Gupta, P. B., Boehm, J. S., Reiling, J. H., Silver, S., Lu, Y., Stemke-Hale, K., Dutta, B., Joy, C., Sahin, A. A., Gonzalez-Angulo, A. M., Lluch, A., Rameh, L. E., Jacks, T., Root, D. E., Lander, E. S., Mills, G. B., Hahn, W. C., Sellers, W. R., and Garraway, L. A. (2009) *Cancer Cell* **16,** 21–32
40. Takeishi, Y., Jalili, T., Ball, N. A., and Walsh, R. A. (1999) *Circ. Res.* **85,** 264–271
41. Lu, Z., Jiang, Y. P., Xu, X. H., Ballou, L. M., Cohen, I. S., and Lin, R. Z. (2007) *Diabetes* **56**, 2780–2789
42. Pochynyuk, O., Tong, Q., Staruschenko, A., and Stockand, J. D. (2007) *J. Physiol.* **580,** 365–372
43. Kwon, Y., Hofmann, T., and Montell, C. (2007) *Mol. Cell* **25,** 491–503
44. Sun, Y., and Rigas, B. (2008) *Cancer Res.* **68,** 8269–8277
45. Laurent, A., Nicco, C., Chéreau, C., Goulvestre, C., Alexandre, J., Alves, A., Lévy, E., Goldwasser, F., Panis, Y., Soubrane, O., Weill, B., and Batteux, F. (2005) *Cancer Res.* **65,** 948–956